DOI: 10.26599/FSHW.2025.9250523

Contents lists available at SciOpen

Food Science and Human Wellness

journal homepage: https://www.sciopen.com/journal/2097-0765

China Food Publishing Co.

Elucidating the molecular mechanism of myofibrillar protein-luteolin affecting lipid accumulation and oxidative stress in HepG2 cells

Zhenyang Wu, Rui Zheng, Xue Zhao*, Xinglian Xu*

State Key Laboratory of Meat Quality Control and Cultured Meat Development, Jiangsu Collaborative Innovation Center of Meat Production and Processing, Quality and Safety Control, College of Food Science and Technology, Nanjing Agricultural University, NO.1 Weigang, Nanjing, Jiangsu, 210095, PR China

ABSTRACT: The luteolin (Lut) binding with myofibrillar protein (MP) can enhance the functionality of proteins, having the potential to ameliorate obesity in the form of dietary intervention. Our previous research unveiled the *in vitro* cell viability and antioxidant properties of the MP-derived and Lut-containing multicomponent peptides (MDLPs). This study aimed to further investigate the effect of MDLPs intervention and downstream effects on lipid metabolism using integrated physiological and multi-omics approaches. The results demonstrated that MDLPs significantly ameliorated steatosis and systemic oxidative stress in HepG2 cells induced by a high-fat (HF) reagent. Combining metabolomic and transcriptomic analysis indicated that PPAR, FoxO, and amino acids metabolism signaling pathways played pivotal roles in response to the MDLPs intervention, primarily through upregulating PPARα, PPARγ, FOXO1, and PLIN4. The abundance of potential disease biomarkers (4-hydroxynonenal and hydroxylinoleic acid) were enhanced. The outcomes of this research provide the theoretical basis for the formulation of novel meat products with anti-obesity activity.

KEYWORDS: myofibrillar protein-luteolin conjugates, lipid accumulation, oxidative stress, multi-omics analysis, HepG2 cells

1. Introduction

Nowadays, the availability of abundant food supplements and the rapid growth of the food manufacturing industry have contributed to unhealthy dietary patterns, such as high-fat diets (HFD)[1]. Prolonged consumption of HFD has been associated with chronic diseases[2], including type 2 diabetes mellitus, cardiovascular disease, and nonalcoholic fatty liver disease (NAFLD), often accompanied by intestinal microflora imbalance and intestinal barrier dysfunction[3]. Meanwhile, the high incidence rate of chronic metabolic diseases was closely related to obesity-mediated inflammatory reactions and oxidative stress[4]. The 2022 Global Nutrition Report underscores the gravity of this issue, revealing that approximately 40% of adults and 20% of children are now overweight or obese. Therefore, promoting healthy lifestyle behavior and early treatment of lipid metabolism disorders was undisputed to mitigate these risks[5]. Lipid loss surgery and various pharmaceutical interventions like fibrates, statins, and resins have demonstrated significant efficacy in

***Corresponding author**
Xue Zhao (zhaoxue@njau.edu.cn), Xinglian Xu (xlxus@njau.edu.cn).

Received 06 October 2024
Received in revised from 26 December 2024
Accepted 13 January 2025

addressing these disorders[6]. At the same time, they may also be accompanied by varying degrees of abnormal blood glucose, myalgia, and other muscle side effects[7]. Studies[8–10] have shown that natural active substances (e.g. polyphenols, saponins, polysaccharides) can regulate lipid metabolism and alleviate lipid accumulation *in vitro* and *in vivo* experiments. Therefore, dietary intervention combining traditional high-lipid meat products (e.g. emulsified sausages and other meat mince products) with natural active substances was an effective strategy for regulating fat metabolism and endowing traditional meat products with new health attributes.

Luteolin (Lut) is a natural food-derived and widely found flavonoid compound with antioxidant, anti-inflammatory, and antibacterial effects[11,12]. Various studies[13,14] have shown that dietary Lut effectively reduces body weight gain and fat deposition in animal experiments. However, due to the poor solubility[15] of Lut and the unpleasant taste[16] under cosolvent solubilization (i.e. ethanol, DMSO, etc.), there are obstacles in its practical application. In the previous study[17,18], we used chicken breast-derived myofibrillar protein (MP) encapsulated Lut combined with high-pressure homogenization technology to obtain the greenly prepared highly loaded MP-Lut vehicle. *In vitro* environment, it was proved that the digested products (MP-derived and Lut-containing digested peptides, MDLPs) have superior *in vitro* antioxidant activity, high cell activity, and alleviated lipid accumulation within a certain concentration (Fig. S1). Notwithstanding the established correlation between MDLPs intervention and alleviation of steatosis, the efficacious therapeutic mechanisms for lipid accumulation remain unclear.

Excessive lipid accumulation can induce oxidative stress in the liver, and the process of steatosis is often accompanied by hepatic oxidative stress[19]. Lipid accumulation and oxidative stress have a mutually reinforcing relationship, contributing to a complex pathological process. Additionally, the increased generation of reactive oxygen species (ROS) has been identified as a key early factor in promoting HFD-induced hyperlipidemia and hyperglycemia[20]. Multi-omics analysis, particularly the combined use of metabolomics and transcriptomics, enables precise examination of the following: (1) changes in vital activities at the gene expression level; (2) qualitative and quantitative analysis of terminal small-molecule metabolites within cells; and (3) target screening and deeper investigation into underlying mechanisms. This approach is widely applied in complex pathological models[21,22]. Transcriptomic analysis had been used to explore bioactive components in *Andrias davidianus* meat[21]. Metabolomics analysis identified vitamin B6 as the key target for green pea hull polyphenol extract in alleviating lipid accumulation in liver cells[8]. Integration of transcriptomics and metabolomics profiling showed that *Rhodomyrtus tomentosa* (Ait.) Hassk fruit phenolic-rich extract can regulate the endotoxin–TLR4–NF-κB pathway to ameliorate steatosis[23]. These findings highlight the potential of multi-omics analysis to explore metabolic pathways and mechanisms involved in MDLPs intervention in lipid metabolism disorders.

This study aimed to further characterize the biological activity of MDLPs in mitigating lipid accumulation and oxidative stress, with an ethanol addition group used for comparison. An *in vitro* HFD-induced HepG2 cell model was employed to assess lipid accumulation and oxidative stress. A

combination of transcriptomics and metabolomics was utilized to explore intervention-related signaling pathways, identify key transcription factors, and examine proteins involved in transcriptional and metabolic regulation. Selected genes and proteins associated with lipid metabolism were validated using real-time quantitative polymerase chain reaction (RT-qPCR) and western blot analysis (WB). The findings from this study are anticipated to offer new insights into the mechanisms by which MP-Lut regulates lipid metabolism, providing a theoretical foundation for the development of anti-obesity functional meat products.

2. Material and methods

2.1. Materials and reagents.

Fresh white feather broiler chicken breast meat was purchased from the local Suguo supermarket, and the chicken samples were kept in an ice bath during transportation. Lut was purchased from McClean Reagent Co., Ltd. (Shanghai, China). High glucose medium DMEM, fetal bovine serum (FBS), and trypsin were purchased from Gibco, USA. DCFH-DA probes were purchased from Biyuntian Biotechnology Co., Ltd. (Nanjing, China). TG detection kit, TC detection kit, and oil red O staining solution were purchased from Nanjing Jiancheng Bioengineering Institute (Nanjing, China). Trizol cell lysis buffer was purchased from Absin Biotechnology Co., Ltd. (Shanghai, China). All reagents used in the experiment were analytically pure.

2.2. MP extraction.

The chicken MPs were extracted as previously described[24]. Briefly, the chicken breast meat was cut into small pieces for crushing (3000 r/min, 20 s) after removing fat and connective tissue. The minced meat was weighed and added with 4 times the volume of standard salt solution (SSS), containing 0.1 M KCl, 20 mmol/L K_2HPO_4 / KH_2PO_4, 1 mmol/L EGTA, and 2 mmol/L $MgCl_2$, and then the mixture was homogenized at 6700 r/min for 1 min using a high-speed homogenizer (Prima, model PD500-TP, UK). Then, the homogenate was filtered through four layers of gauze, and the filtrate was centrifuged at 2000 g at 4℃ for 10 min (Avanti JE, Beckman Coulter, United States). The supernatant was discarded, the crude MP precipitate was collected, and the above process was repeated twice. Subsequently, the precipitate was homogenized with four times the volume of 0.1 M KCl solution at 6700 r/min for 1 min, centrifuged at 2500 g at 4℃ for 10 min, and then repeated to remove impurities and obtain pure MP. The protein content of MP was determined by the biuret method. MP was used within 3 days.

2.3. Preparation of MDLPs.

MDLPs were produced based on our previous method[17]. Briefly, MP suspension was diluted with phosphate buffer solution (PBS, 0.6 M NaCl, 50 mmol/L K_2HPO_4 / KH_2PO_4, pH 7, the same as below) to a concentration of 10 mg/mL. Then the solution underwent pre-homogenization treatment with the high-speed homogenizer. The obtained pre-homogenized solution was subjected to high-pressure homogenization treatment (HPH) of 103 MPa pressure. Lut powder was dissolved in anhydrous ethanol / PBS and mixed evenly (ethanol accounted 30%, minimum concentration for promoting dissolution). The stock solution was mixed with MP suspension at different addition amounts to obtain the required Lut concentration. All the

samples were treated by HPH to obtain ethanol-containing / ethanol-free MP-Lut samples. Then samples were treated with *in vitro* gastrointestinal digestion and freeze-drying, obtaining the MDLPs-eth and MDLPs samples. The MTT method was used to determine the cytotoxicity (Fig. S1).

2.4. Cell culture and treatment.

HepG2 cells (10^5 cells) were cultured in DMEM supplemented with 10% FBS and 100 μg/mL penicillin and streptomycin at 37°C in 5% CO_2 and 100% humidity atmosphere. Then, cells were subcultured when the cells became 75%−85% confluent. HepG2 cells (1×10^6 cells/well) were seeded in six-well plates in the complete medium for 24 h (reaching > 80% confluences). Then, the steatosis induction was operated based on the previously reported method[25]. After 24 h of culture, the cells were incubated with High-fat (HF) reagent ($C_{sodium\ oleate}/C_{sodium\ palmitate}$ = 2/1) to establish the model. After the induction, the medium containing MDLPs-eth and MDLPs samples was added. The blank Con group was only cultured with serum-free DMEM medium for the same time. The samples were divided into four groups according to different treatments.

A: Control / wild type (Con / WT) group;

B: HF induction (Ind) group;

C: HF induction + MDLPs-eth (Eth) group;

D: HF induction + MDLPs (Non) group.

2.5. Biochemical assays.

Triglycerides (TG), total cholesterol (TC), and oil red O staining were measured using assay kits following the instructions of the manufacturer. DCFH-DA probe was used to detect reactive oxygen species, and the level of oxidative stress in cells can be judged according to the fluorescence intensity. The operation was as follows: the cells were washed twice with DMEM incubated at 37°C and added a medium-diluted probe (6-well plate, probe concentration of 10 μmol/L) incubating at 37°C for 30 min, and then the cells were washed twice with DMEM to remove the excess probe. The cells were immediately washed with PBS at 37°C. The inverted fluorescence microscope was used to compare the intracellular ROS free radical scavenging, and the fluorescence intensity was detected by ImageJ software quantification.

2.6. Omics analysis.

RNA extraction and hepatic transcriptome analysis. Total RNA was isolated from each group of cell samples using trizol lysis buffer, followed by purification, reverse transcription and sequencing. The library was constructed by Shanghai Baipu Biotechnology Co., Ltd. (Shanghai, China) (Reference genome: Homo_sapiens.GRCh38.dna.primary_assembly. fa). The quality of the library was tested with Agilent 2100 Bioanalyzer, and then the total concentration of the library and the effective concentration of the library were detected. The samples were extracted by RNA. Next-generation sequencing (NGS) was used after extraction, purification, and database construction. Paired-end (PE) sequencing was performed on these libraries based on the Illumina sequencing platform. Adopted DESeq was used to analyze the difference in gene expression, and the conditions for screening differentially expressed genes were as follows: expression difference multiples.

|log2FoldChange| > 1, significant *P*-value < 0.05. The DEGs were annotated and enriched by the Gene Ontology database (GO) and Kyoto Encyclopedia of Genes and Genomes (KEGG) database.

Untargeted hepatic metabolome analysis. The collected cell samples were thawed at 4℃, and 200 μL of pre-cooled water and 800 μL of pre-cooled methanol were added. Mixing and ultrasonic in the ice bath for 20 min, -20℃ incubation for 1 h to precipitate protein, 16000 g centrifuged at 4℃ for 20 min, and the supernatant was taken. During the entire LC-MS / MS analysis, the samples were placed in a 4℃ autosampler. The samples were analyzed by SHIMADZU-LC30 ultra-high performance liquid chromatography (UHPLC) using an ACQUITYUPLC®HSS T3 (2.1 mm × 100 mm, 1.8 μm) (Waters, Milford, MA, USA) chromatographic column. The injection volume was 4 μL, the column temperature was 40℃, and the flow rate was 0.3 mL/min. Chromatographic mobile phase A: 0.1% formic acid aqueous solution, B: containing 0.1% methyl. Acidic acetonitrile solution; the chromatographic gradient elution procedure was as follows: (0-2) min, 0 B; (2-6) min, B from 0% line; sexual changes to 48%; (6-10) min, B from 48% linear change to 100%; (10-12) min, B maintained at. 100%; The structural identification of the metabolites was performed by accurate mass number matching (mass tolerance < 10 ppm) and secondary spectrum matching (mass tolerance < 0.01 Da). Public databases such as HMDB, MassBank, GNPS, and the self-built reference metabolite standard library (BP-DB) were searched. Integrated transcriptome and metabolome analysis were conducted using iPath 3.0 to profile significantly altered metabolic pathways.

2.7. RNA Extraction and RT-qPCR.

Total RNA was isolated from the the collected cell samples using an RNA extraction kit (MiniBEST Universal, TaKaRa, Kusatsu, Shiga, Japan) and reversely transcribed into cDNA using the PrimeScript RT Master Mix (TaKaRa, Kusatsu, Shiga, Japan) according to the recommended procedures. Real-time PCR was performed using the SYBR Premix Ex TaqTM (Tli RnaseH Plus) qPCR kit (TaKaRa, Kusatsu, Shiga, Japan) according to the manufacturer's protocols. The mRNA level of β-actin was used to normalize the relative amount of each measured mRNA, and the $2^{-\Delta\Delta Ct}$ method was chosen to analyze the relative gene expression. Primer sequences are listed in Table S1.

2.8. WB Analysis.

Total proteins of HepG2 cells were extracted using RIPA lysis buffer supplemented with 1% phenylmethylsulfonyl fluoride (PMSF, Thermo Fisher Scientific, MA, USA). Protein concentration was measured using Pierce BCA Protein Assay Kit (23 225, Thermo Fisher Scientific, MA, USA). Proteins (20 μg) were separated on 4%–12% SDS-PAGE gels and transferred to polyvinylidene difluoride membranes (PVDF, 0.22 μm). The PVDF membranes were blocked with 5% bovine serum albumin for 1 h and then blotted with specific primary antibodies (PPAR-α and PPAR-γ), followed by incubation with secondary antibodies. The individual protein bands were visualized by enhanced chemiluminescence with a gel imager (ImageQuant LAS4000, GE Healthcare, IL, USA). The band intensities were quantified by Quantity One (Version 4.6.2, Bio-Rad, CA, USA).

2.9. Statistical analysis.

The raw data of the test were preprocessed by simple calculation, and SPSS 27 software was used for statistical analysis. The t-test was used to compare the mean between the sample groups, and the one-way analysis of variance was used to compare the multiple groups of samples. ANOVA analysis, $P < 0.05$ indicated that the difference was significant, and the results were expressed as mean ± standard deviation (mean ± SD).

3. Results

3.1. Amelioration of MDLPs on HF-induced cell steatosis and oxidative stress.

After HF-induced steatosis, the ROS content in the HF-induced group increased approximately 10-fold in fluorescence intensity (Fig. 1A and 1D). Compared with the Con group (the content of TG and TC was (0.12 ± 0.03) mmol/g pro and (0.06 ± 0.01) mmol/g pro, respectively), the levels of TG (0.31 ± 0.04) mmol/g pro) and TC (0.26 ± 0.02) mmol/g pro in the Ind group were also significantly increased ($P < 0.05$) (Fig. 1B and 1C). Cell viability significantly decreased ($P < 0.05$) at MDLP concentrations of 10.00 mg/mL, indicating substantial damage to HepG2 cells (Fig. S1). Therefore, the optimal concentration was established as 3.00 mg/mL. MDLPs intervention alleviated cellular lipid accumulation and oxidative stress phenotype (Fig. 1D and 1E). Compared with the Ind group, the contents of ROS, TG, and TC decreased by 76.09%, 50.15%, 70.76%, and 80.24%, 50.87%, 72.63% in the Eth and Non groups, respectively, indicating that MDLPs treatment had a significant effect on alleviating HepG2 cell damage.

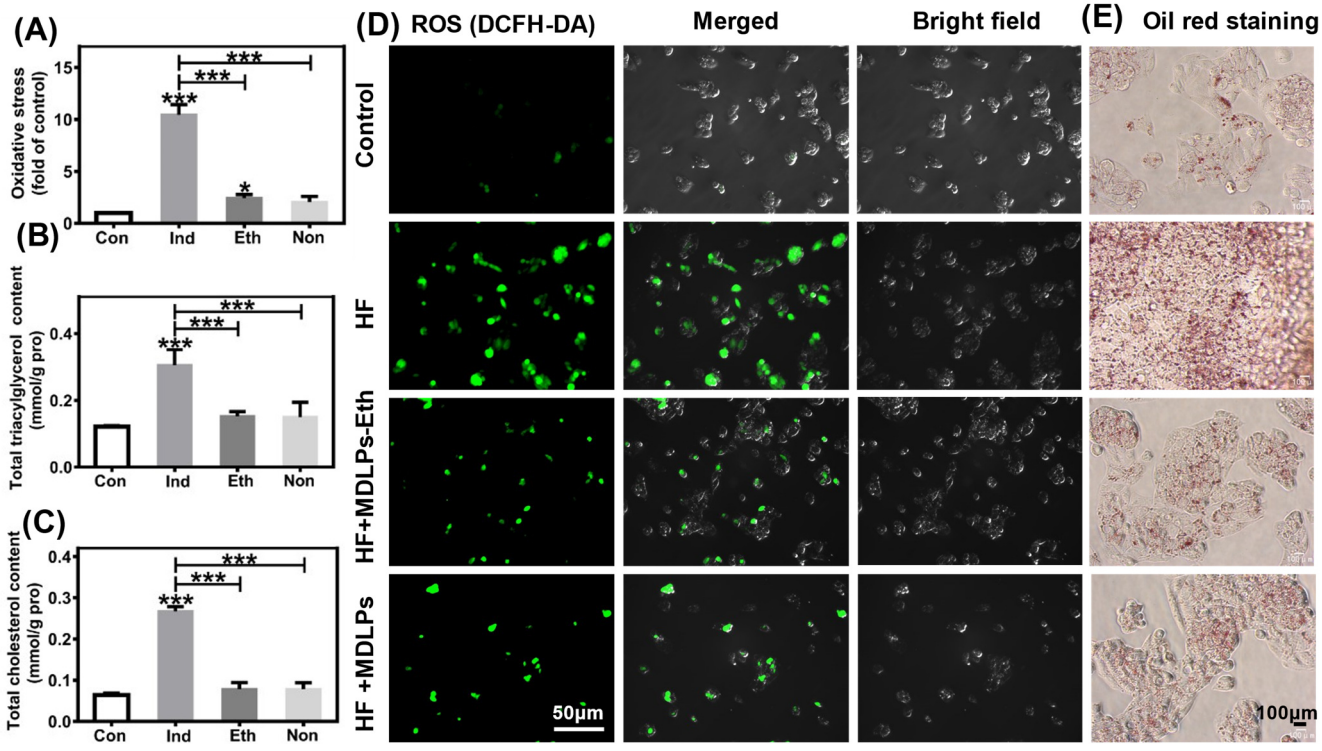

Fig. 1 The (A) oxidative stress level (relative fluorescence intensity of DCFH-DA), (B) total triacylglycerol, (C) total cholesterol, (D) ROS fluorescence (bar = 100μm), and (E) oil red staining images of HepG2 cells after being treated with MDLPs. *above column plots indicate significant difference between means (* = $P < 0.05$, ** = $P < 0.01$, *** = $P < 0.001$).

3.2. Effects of MDLPs supplementation on metabolic profiles.

Metabolomics analysis. Non-targeted metabolomic analysis of the Eth and Non samples revealed the material basis of MDLPs in alleviating lipid accumulation[26]. Significant differences in metabolites between different treatment groups (WT vs. Ind, Ind vs. Eth, and Ind vs. Non) were identified using UPLC-MS/MS analysis. The results showed that the numbers of significantly different annotated metabolites in the three comparison groups were 199, 376, and 307, respectively. PCA analysis indicated the differences between groups, and clustering was confirmed by OPLS-DA (Fig. 2A-B). These findings suggest significant differences in metabolite levels between different treatment groups and highlight potential intracellular biomarkers following MDLPs intervention.

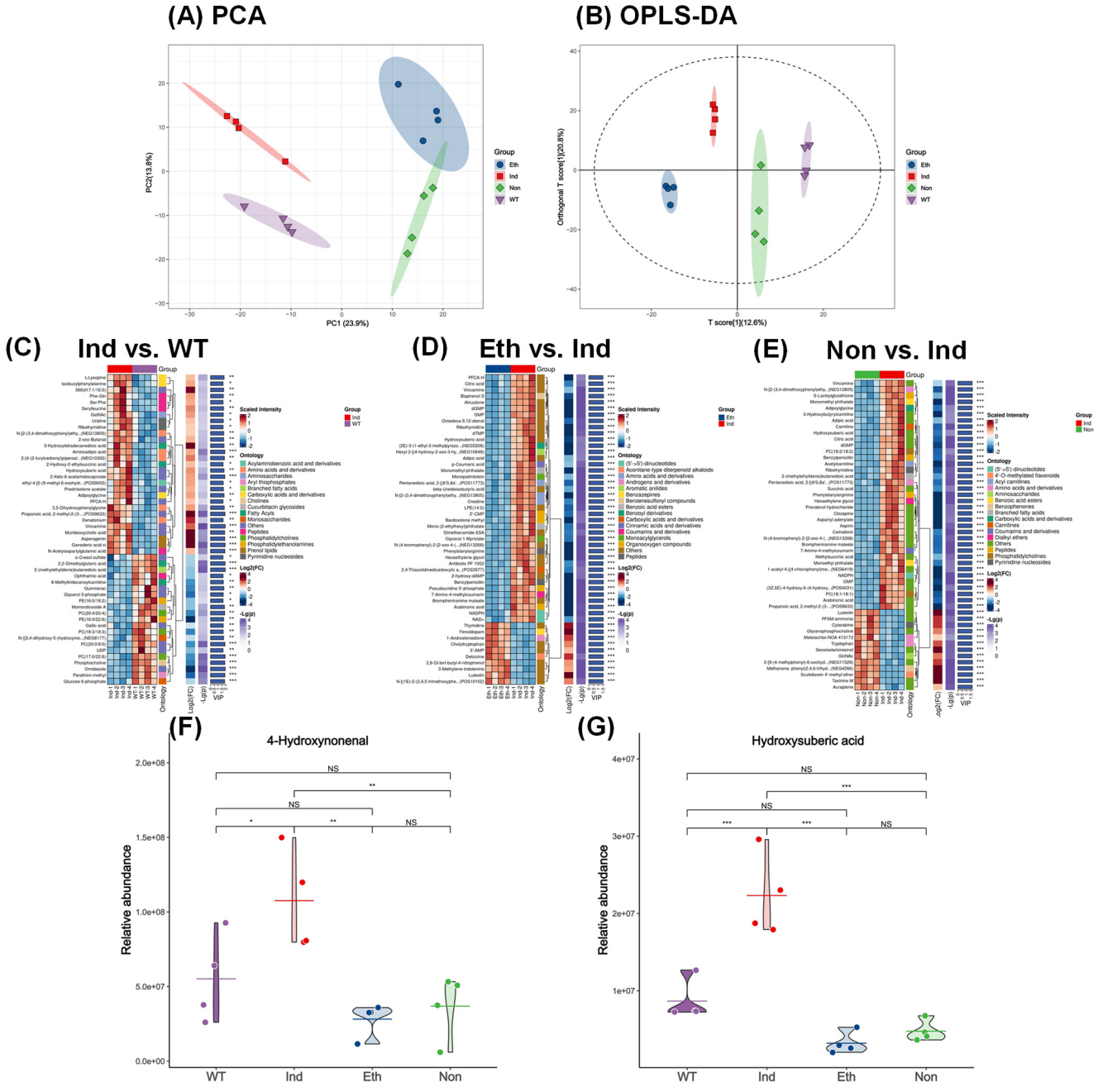

Fig. 2 Effects of MDLPs supplementation on HepG2 cell metabolome. (A) PCA plot, (B) OPLS-DA plot, and VIP scores analysis of (C) WT vs. Ind, (D) Ind vs. Eth, and (E) Ind vs. Non groups. (E) Selected potential metabolites biomarkers. *above column plots indicate significant difference between means (* = $P < 0.05$, ** = $P < 0.01$, *** = $P < 0.001$).

The PCA results were compared in multiple groups, the results showed that the first principal component accounted for 23.90% of the total variance in the comparison, and the second principal component accounted for 13.8%. In the comparison between the two groups (WT vs. Ind, Ind vs. Eth, and Ind vs. Non groups), the first principal component accounted for 27.50%, 42.30%, and 35.10% according to OPLS-DA and Score-plot analysis. The corresponding Q^2 values of the three comparison groups were 0.734, 0.963, and 0.883, respectively, indicating the reliability of the established model (Fig. S2). The results of differential metabolites showed that potential biomarker metabolites included fatty acids (hydroxylinoleic acid, glycerol 3−phosphate, glycerol phosphate), carboxylic acids (methyl succinic acid, adipic acid, 2-isopropylmalic acid, arabic acid, monomethyl phthalate, 3-hydroxy dodecane dioic acid, 3-hydroxytetraenedic acid, tetraenedic acid, polyethylene glycolic acid), amino acids (acetyl-L-threonine, tyrosine, fatty acyl glycine), phenolic acids (gallic acid, hesperidin), and nucleotides (thymine ribonucleoside). The content of 4-hydroxynonenal and hydroxylinoleic acid (Fig. 2E-F) showed the tendency to return to normal levels after HF-induction, which can reflect the impact of MDLPs intervention. In the expression profile of metabolites with higher importance (VIP value is the top 50, VIP score > 1.5), there were significant differences in metabolites among the WT vs. Ind, Ind vs. Eth, and Ind vs. Non groups (Fig. 2C-E). Compared with the Con group, among the 50 metabolites in the induction group (Fig. 2C), the main categories were acylaminobenzoic acid and its derivatives, amino acids and their derivatives, lipids, pyrimidine nucleosides, phosphatidylcholine. In the Ind vs. Eth group, the VIP expression profile of metabolites was similar to that of the Ind vs. Non group, mainly (5'−>5')-dinucleotides, 4'-O-methylated flavonoids, acylcarnitine, amino acids, and its derivatives, branched-chain fatty acids, carboxylic acids and its derivatives, carnitine, coumarin and its derivatives, peptides, phosphatidylcholine, pyrimidine nucleosides. It was worth noted that more phenolic acid class metabolites were annotated in the Ind vs. Eth group, while there was 4' -O-methylflavonoidization in the Ind vs. Non group, indicating that ethanol may affect Lut metabolism during digestion or intracellular transport.

Metabolomics KEGG enrichment analysis. In order to explore the most significant biological processes in the metabolism of intracellular substances after MDLPs intervention, the differential metabolites in the three comparison groups (Con vs. Ind, Ind vs. Eth, Ind vs. Non) were annotated to 33, 40, and 35 pathways, respectively. (Fig. 3). The most representative functional categories of KEGG enrichment analysis were global and overview maps, followed by amino acid metabolism, lipid metabolism, membrane transport, digestive system, cancer metabolism, and biosynthesis of other secondary metabolisms such as carbohydrates. KEGG enrichment analysis showed that the differential metabolites in the three comparison groups after MDLPs intervention were mainly distributed in the environmental information processing: Signal transduction category (subclasses included: 5 and 17, respectively, 9 pathways); Metabolism: Global and Overview Atlas (subclasses include: 46, 94, 82 pathways), Amino acid metabolism (subclasses include:18,31,36 pathways), other secondary metabolite synthesis categories (subclasses include: 12, 30, 21 pathways); Human biological systems: digestive system (subclasses include: 12, 30, 22 pathways), Endocrine system categories (subclasses include:2, 15, 12 pathways). It was worth noting that amino acid metabolism

plays a crucial role in KEGG enrichment analysis, particularly when considering the intersection between amino acid and lipid metabolism within energy metabolism. For instance, leucine and isoleucine can be converted to acetyl-CoA after deamination[27]. The digested amino acid metabolites of MP may enter the tricarboxylic acid (TCA) cycle or act as precursors for fatty acid synthesis, directly contributing to the regulation of lipid metabolism in lipid-accumulating HepG2 cells.

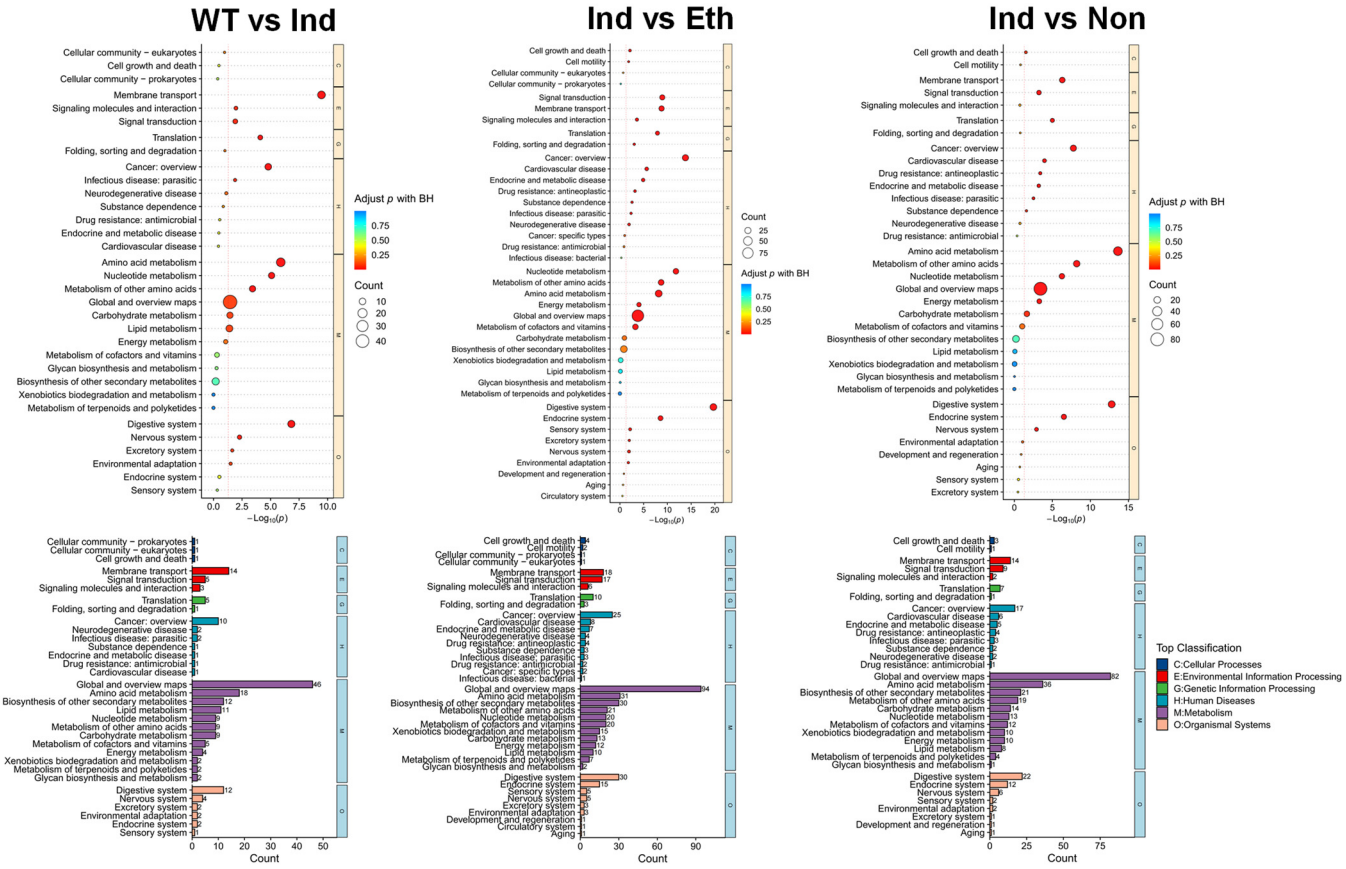

Fig. 3 Bubble and category bar diagram of enriched KEGG pathways. The size of the dots represents the number of metabolites in each KEGG pathway, the top-level classification of the bar color pathway, where the x-axis represents the number of metabolites.

3.3. Effects of MDLPs supplementation on transcriptome.

Transcriptome analysis. Fig. 4A presents the PCA analysis results for the various groups. Significant differences in gene expression levels were observed among the different treatment groups, while the replicate samples exhibited high similarity. Notably, the Eth and Non groups demonstrated a strong similarity compared to the Con and Ind groups, primarily due to the similar treatment conditions, with the only difference being the presence of co-solvents.

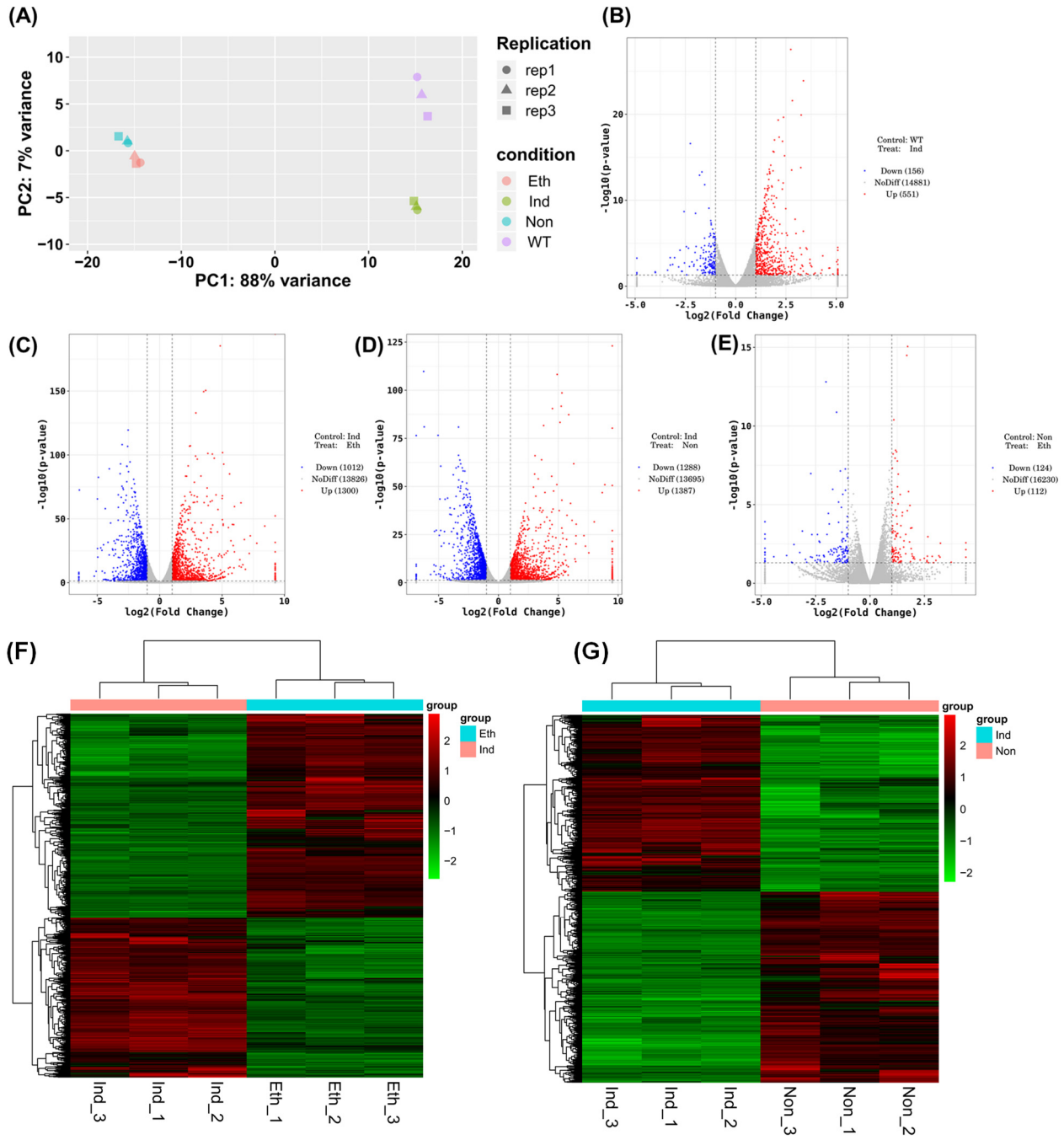

Fig. 4 (A) Pearson correlation coefficient test. Transcriptomic analysis of differentially expressed gene volcano plots in different treatment groups (DESeq2, |log2FoldChange| > 1, *Q*-value < 0.05) (B) WT vs. Ind, (C) Ind vs. Eth, (D) Ind vs. Non, (E) Eth vs. Non. Cluster analysis of (F) Ind vs. Eth and (G)Ind vs. Non groups.

The expression of the HepG2 gene in different treatment groups was analyzed using transcriptomics to investigate the mechanisms by which MDLPs-Eth and MDLPs interventions alleviate cellular lipid accumulation. As shown in Fig. 4, the analysis was conducted using DESeq2 (*Q* value < 0.05). In the Con group, 707 differential genes were identified, with 551 upregulated and 156 downregulated. Compared to the Ind group, 2312 differential genes were identified in the Eth group (1300 upregulated and 1012 downregulated) and 2675 in the Non group (1387 upregulated and 1288 downregulated). Additionally, 236 differential genes were identified between the Eth and the Non groups, with 112 upregulated and 124 downregulated. HF induction treatment significantly affected gene expression at the transcriptional level in

HepG2 cells in the Con group (Fig. 4B). After MDLPs-Eth and MDLPs interventions, cellular steatosis was effectively alleviated, and more differential genes were detected at the transcriptional level in the Eth and Non groups (Fig. 4C-D). The comparison between the Eth and Non groups showed minimal differences in gene expression (Fig. 4E). Cluster analysis was used to identify expression patterns of differentially expressed genes under various conditions, with clustering of differentially expressed genes in the Ind vs. Eth and the Ind vs. Non groups shown in Fig. 4G-H. Key DEG expression levels were quantitatively analyzed (Fig. S3). Key genes involved in mitochondrial oxidative phosphorylation, such as ATP4A, NDUFS7, and ATP6V0A4, were upregulated by 6.83/4.44 times ($P < 0.01$), 1.89/3.25 times ($P < 0.01$), and 8.33/7.05 times ($P < 0.01$), respectively. Key genes involved in glycerol phospholipid metabolism, such as MBOAT1 and PLPP2, were upregulated by 0.57/1.94 times and 3.01/3.66 times, respectively, indicating significant effects on intracellular energy metabolism after MDLPs intervention. Mitochondrial oxidative phosphorylation plays a crucial role in the β-oxidation of fatty acids, and its dysfunction can result in lipid accumulation and metabolic disorders[28], such as fatty liver and obesity. Consequently, MDLPs intervention may influence oxidative phosphorylation products (e.g., ATP/NADH ratio), thereby regulating metabolic signaling pathways such as mTOR and AMPK, which affect lipid synthesis and fatty acid degradation[29]. Additionally, the regulation of glycerophospholipid metabolism may impact fatty acid oxidation and ATP production by modulating mitochondrial function, thus mitigating lipid accumulation.

Transcriptome KEGG enrichment analysis. According to the results of KEGG enrichment analysis of differentially expressed genes, the top 30 genes with the most significant enrichment (the smallest p-value) were screened (Fig. 5). These differential genes are mainly classified into five parts: cell process, environmental information processing, genetic information processing, human disease, and metabolism. Differential genes between the Con and Ind groups were mainly involved in focal adhesion, p53 signaling, TGF-β signaling, PI3K-Akt signaling, ECM receptor interaction, butyric acid metabolism, protein digestion, and absorption, linoleic acid metabolism, cholesterol metabolism, PPAR signaling, and the metabolism and synthesis of various amino acids including glycine, serine, and threonine. Following MDLPs intervention, multiple amino acid metabolic pathways, along with the PPAR and FoxO signaling pathways, were significantly enriched in both the Eth and Non groups, exhibiting high abundance and a low false discovery rate (FDR). Additional pathways enriched in the treatment groups included linoleic acid metabolism (Eth), fatty acid degradation (shared), glyceride metabolism (shared), glycolysis/gluconeogenesis (shared), biosynthesis of unsaturated fatty acids (shared), cholesterol metabolism (Non), and fat digestion and absorption (Non). These signaling pathways may collectively contribute to the beneficial effects of MDLPs on lipid accumulation. Variations in the enrichment of lipid metabolism-related pathways suggest distinct roles for the two treatment groups in reducing cellular lipid accumulation.

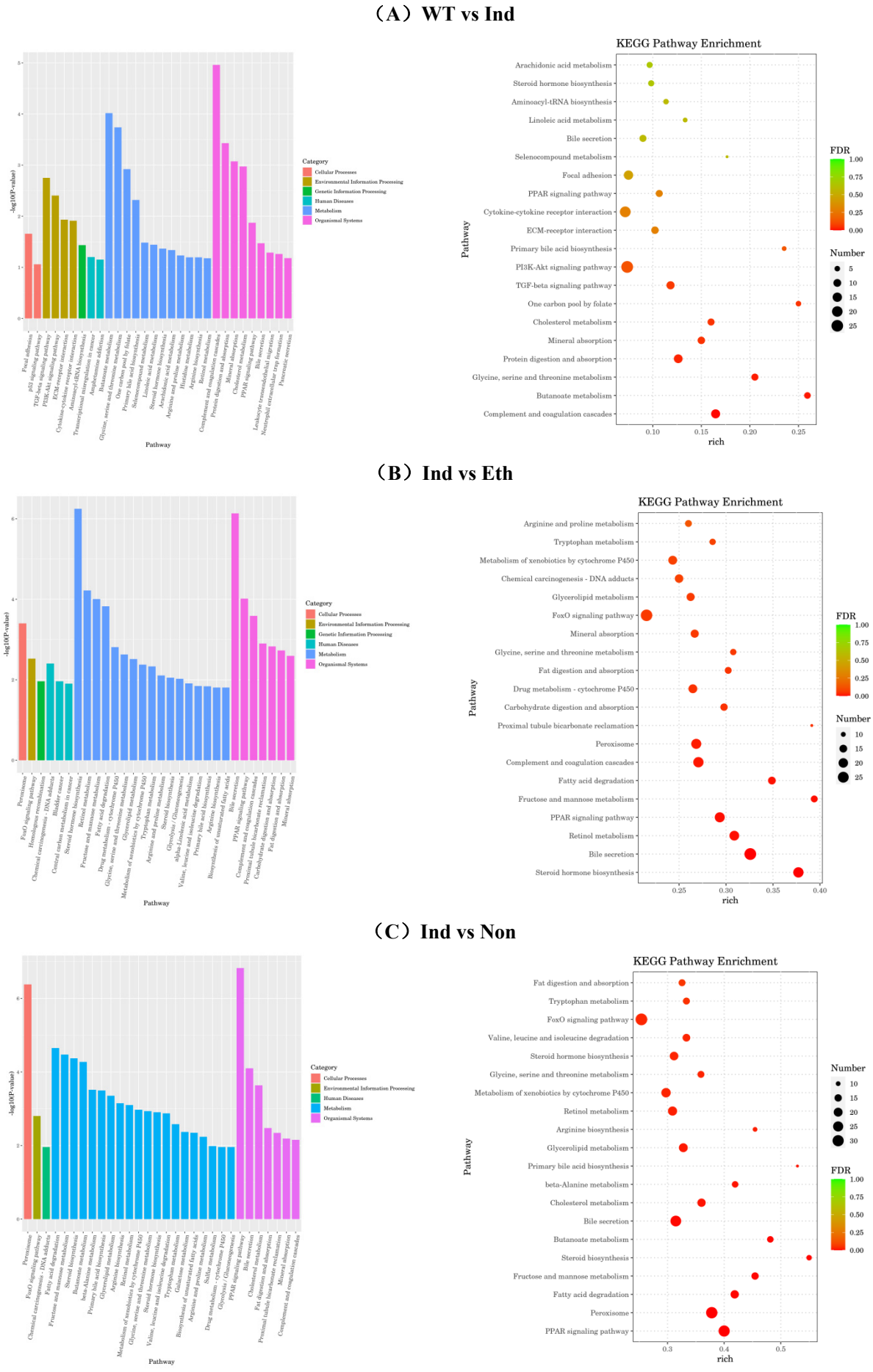

Fig. 5 Transcriptomic analysis of differentially expressed gene. The KEGG classification analysis (level 2) and KEGG enrichment analysis in (A) WT vs Ind, (B) Ind vs Eth, (C) Ind vs Non, and (D) Eth vs Non groups.

3.4. Protein-protein interactive (PPI) analysis.

In the classification of transcriptome differential genes, the number of genes related to lipid metabolism was higher than that of amino acid metabolism and carbohydrate metabolism, indicating that HF-induced lipid accumulation. The MDLPs-Eth and MDLPs interventions primarily affected lipid metabolism and also influenced carbohydrate metabolism in cells.

The protein-protein interaction network analysis was performed on the proteins corresponding to the differentially expressed genes with high expression levels (|log2FoldChange| > 2 or activated genes) in the omics results to screen possible hub proteins[30]. After analyzing the 2313 (Ind vs. Eth) and 2676 (Ind vs. Non) involved targets through the string database, linkages between different targets were established (Fig. 6A and B). Using the CytoHubba algorithm in the Cytoscape application, a minimum interaction score of 0.700 (high confidence) was set for the network. Key proteins (degree < 10) corresponding to differential genes were identified (Fig. 6C and D). It was worth noting that IL-6 (Ind vs. Eth) and COL1A1, COL1A2 (Ind vs. Non) were most closely linked to other genes, implying that the intervention of MDLPs may affect the expression of inflammatory cytokines, chemokines, and profibrotic genes. Lipid accumulation or fatty acid oxidation defects are associated with increased lipotoxicity, which directly leads to the development of fibrosis, and a variety of fibrosis factors also change the process of lipid metabolism[31]. The above results indicated that MDLPs intervention involved cytokine regulation, hepatocyte fibrosis, and other processes, which need further exploration.

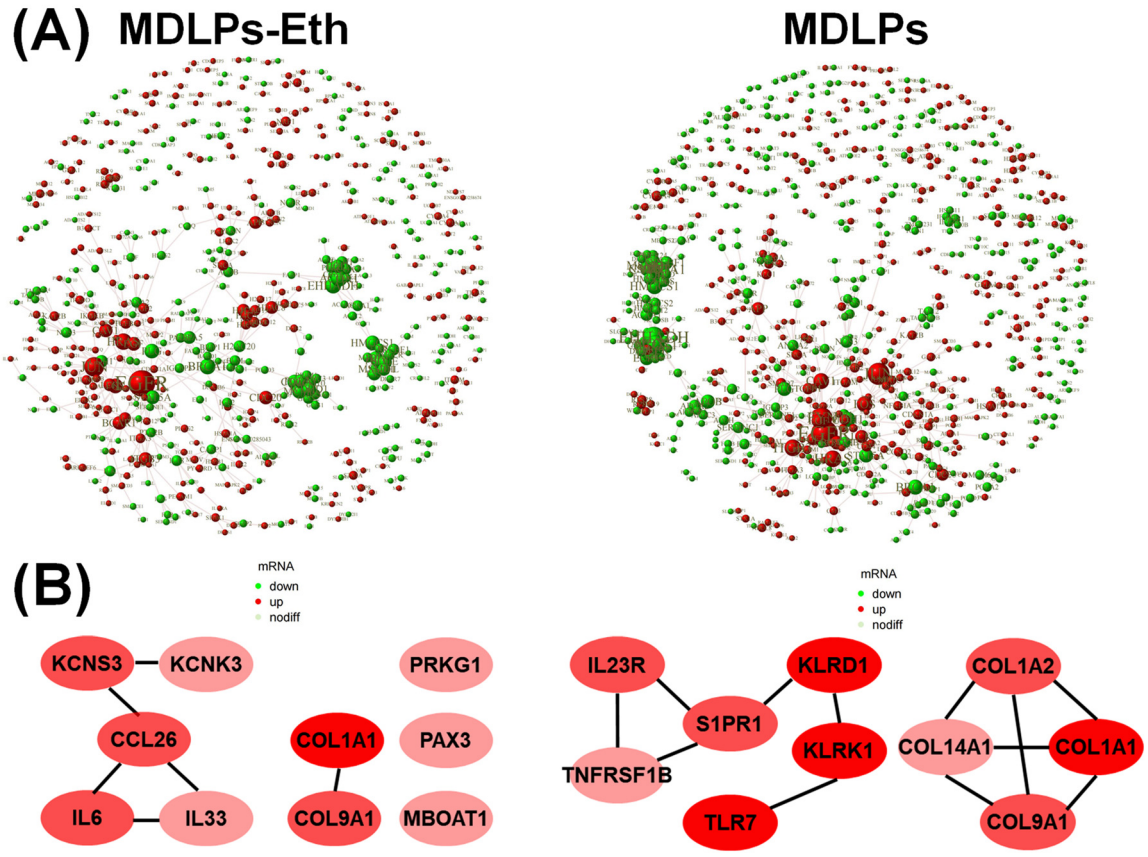

Fig. 6 (A) PPI analysis and (B) hub protein screening of Ind vs. Eth and Ind vs. Non. Setting: hiding disconnected nodes in the network and the minimum required interaction score > 0.700 (high confidence).

3.5. Integrated analysis of transcriptome and metabolome in lipid metabolism.

To further consolidate these findings, we performed an in-depth analysis of key DEGs and metabolites involved in glycerophospholipid metabolism, glycerolipid metabolism, as well as fatty acid biosynthesis and degradation. By integrating differential metabolites (VIP > 1, $P < 0.05$) and DEGs (|log2FoldChange| > 1, $P < 0.05$) in iPath 3.0 to further explore the changes in metabolic pathways after MDLPs intervention (Fig. 7). The pathways that exhibited changes in Ind vs. Eth and Ind vs. Non groups were mainly enriched in lipid metabolism and energy metabolism, as shown in the Sankey diagram (Fig. 8). This analysis indicated that MDLPs primarily regulate substance metabolism in both Eth and Non groups. Comprehensive transcriptome and metabolome analyses suggest that MDLPs may alleviate steatosis by modulating energy production and lipid metabolism pathways. As shown in Fig. 9A, the effects of MDLPs in mitigating lipid metabolism disorders and their underlying mechanisms are summarized. MDLPs intervention primarily remodels lipid droplets and enhances lipid droplet-mitochondrial interactions, which upregulates the expression of Plin4, promotes mitochondrial lipid oxidation, regulates energy metabolism, and mitigates lipid toxicity. Based on integrated omics analysis, the PPAR pathway appears to play a key role in regulating lipid metabolism. To validate the results of the multi-omics analysis, we analyzed the mRNA expression levels of FA metabolism-related genes and PPAR pathway-related proteins. The results (Fig. 9B) showed that MDLPs intervention significantly reversed HF-induced downregulation of PPARα, PPARγ, FOXO1, and PLIN4. Following MDLPs intervention, the low expression levels of PPARα protein induced by HF conditions were also reversed, and PPARγ protein expression was activated. The PPARα and PPARγ protein content in both the Eth and Non groups was significantly higher compared to the Ind group ($P < 0.05$). It was worth noting that transcription and expression are not linearly strongly related. Considering that from transcriptome to proteome, there is a complex and intricate translational regulatory stage. The abundance of proteins in cells is mainly controlled by translation levels, and proteins may have significant differences from mRNA in terms of half-life, synthesis rate, and quantity[32].

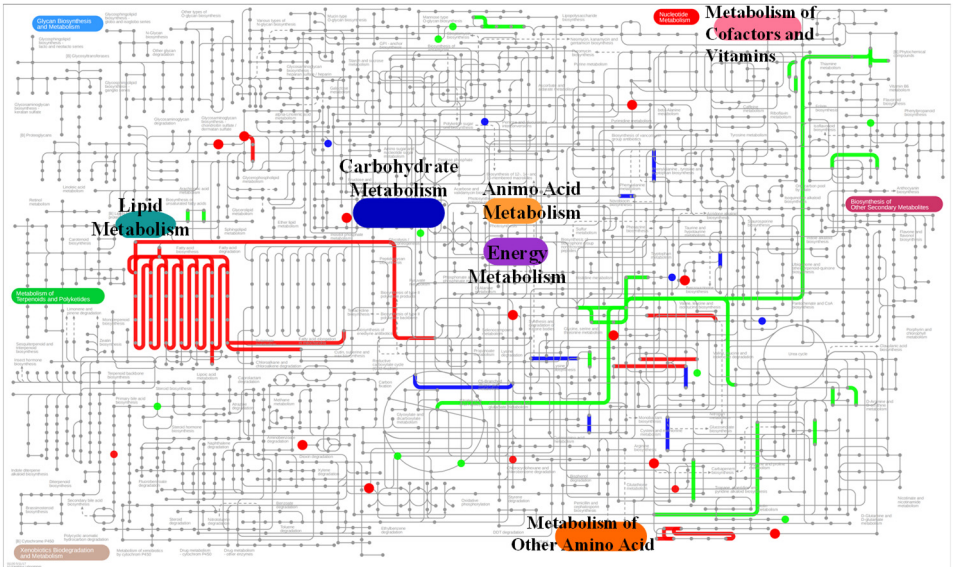

Fig. 7 Integrated transcriptome and metabolome analysis in iPath 3.0 for visualizing KEGG general metabolic pathway map. Dots and lines represent differential metabolites and DEGs, respectively. Red, WT vs. Ind; green, Ind vs. MDLPs; blue, shared metabolites and DEGs.

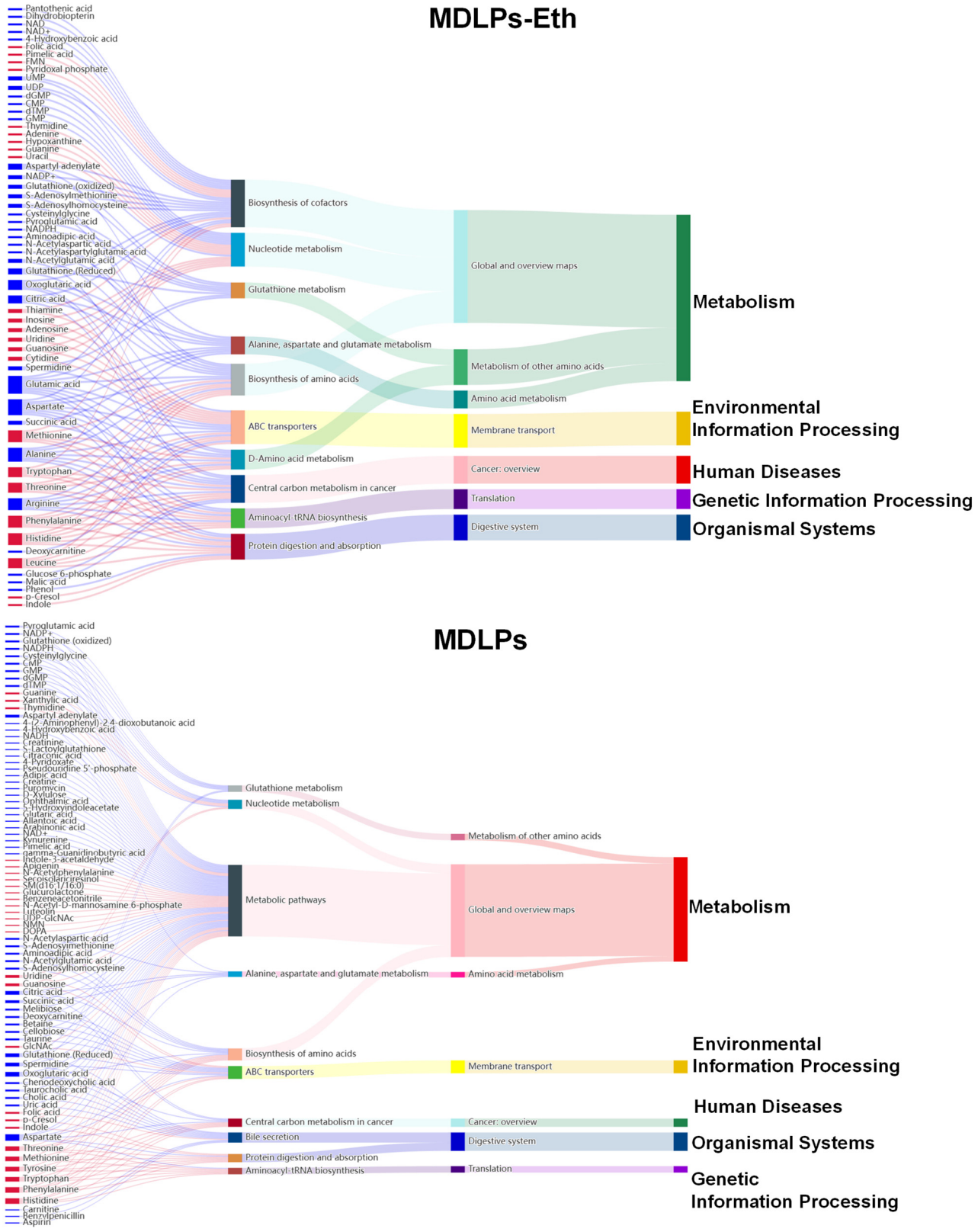

Fig. 8 Sankey diagram of differential metabolites in Ind vs. Eth, Ind vs. Non groups, showing the relationship between the pathways enriched with significant-top 10 and differential metabolites. From left to right are the differential metabolites, the metabolic pathways significantly enriched ($P < 0.05$), the second layer KEGG pathway category, and the top KEGG pathway category.

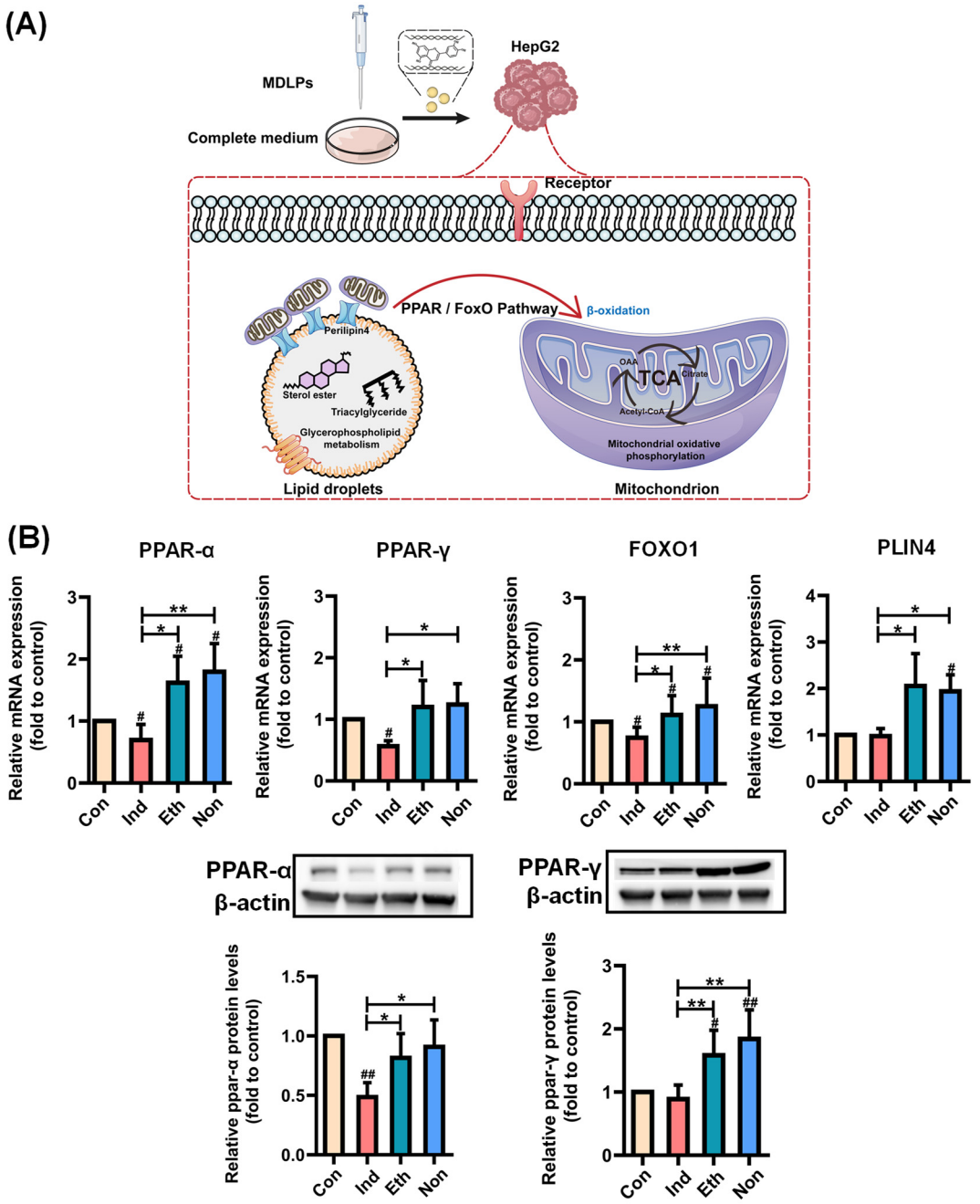

Fig. 9 (A) Schematic diagram showing the mechanisms of MDLPs on ameliorating HepG2 cells steatosis, (B) RT-qPCR results of metabolism-related genes and protein expression levels. $^{\#}P < 0.05$, $^{\#\#}P < 0.01$ were compared between the Con and other groups.

4. Discussion

In this study, we investigated the effects of different MDLPs treatments on HF-induced steatosis in HepG2 cells. After intervention with MDLPs at a concentration of 3 mg/mL, intracellular lipid droplet morphology significantly improved, and there was a notable decrease in total triglyceride and cholesterol content, indicating the alleviation of cellular lipid accumulation. Additionally, intracellular ROS content significantly decreased, suggesting that MDLPs exert their effects by regulating lipid metabolism and oxidative stress. Consistent with previous studies[33,34], nobiletin and curcumin also alleviated lipid deposition and oxidative stress in steatosis-induced HepG2 cells. Notably, the effects of Eth and Non samples on cellular

DEGs and differential metabolite abundances were generally consistent. The PPAR pathway and fatty acid metabolism pathway were common to both groups in the KEGG enrichment analysis of the transcriptome. However, differences in specific intracellular metabolites were observed, such as higher flavonoid content in the Non group. Considering the complex regulation of transcriptional expression of intracellular signal factors, MDLPs-Eth and MDLPs exhibited similar effects in alleviating steatosis and preventing cell damage.

To further explore the ameliorating effect of MDLPs on hepatocyte-related metabolic processes, transcriptomic analysis was performed. GO terms (regulation of steroid metabolism, fatty acid metabolism, intracellular lipid metabolism, and lipid lysis) and KEGG pathways (linoleic acid metabolism, fatty acid degradation, glyceride metabolism, biosynthesis of unsaturated fatty acids, and cholesterol metabolism) indicated that MDLPs may alleviate cellular steatosis by regulating genes involved in lipid metabolism. In the pathways involved in the distribution of DEGs, the focal adhesion signaling pathway, which regulates cell adhesion and differentiation, involved MAPK, PI3K/Akt, and Rho pathways[35]. The p53 signaling pathway, closely related to cell cycle regulation and cancer prevention, showed a significant correlation between the R72 mutation of p53 and weight gain, as well as susceptibility to type II diabetes mellitus[36]. The PPAR and FOXO signaling pathways were common enrichment pathways in Ind vs. Eth and Ind vs. Non groups. The liver's three fatty acid oxidative metabolism pathways, mitochondrial β-oxidation, peroxisome β-oxidation, and microsomal/endoplasmic reticulum omega-oxidation are mainly regulated by PPARα[37,38]. PPARβ/δ also participates in regulating some enzymes[39]. Downregulate PPARγ may inhibit liver lipogenesis, upregulate PPARα, promote β-oxidation, and reduce lipid synthesis[40], and thus improve NAFLD symptoms. Studies[37,41] have shown that activating PPARα in the liver decreases triglyceride levels and increases high density lipoprotein levels, suggesting a potential therapeutic strategy for lipid accumulation. Oxidative stress is linked to steatosis and inflammation during steatosis development[33]. FOXO proteins regulate antioxidant gene expression, enhancing the cell's antioxidant capacity and scavenging free radicals, potentially explaining the oxidative stress resistance observed with MDLPs intervention[42,43].

An imbalance between nutrient intake and energy expenditure contributes to lipid metabolism disorders, oxidative stress, and chronic inflammation[10]. Metabolomics analysis helps explore molecular mechanisms of lipid metabolism disorders and identify metabolic markers, reflecting disease processes[44]. HF-induced significant intracellular lipid accumulation, with increased biomarkers like 4-hydroxynonenal and hydroxylinoleic acid in the Ind group. Hydroxylinoleic acid was an oxidation product of polyunsaturated fatty acids (e.g., linoleic acid) formed in a free radical-mediated lipid peroxidation reaction[45] and acts as an intracellular signaling molecule in lipid metabolism to affect cellular function by activating or inhibiting specific signaling pathways, such as through binding PPARs as well as cell surface receptors to regulate lipid metabolism and inflammatory responses[46]. 4-Hydroxynonenal, a lipid peroxidation product, indicates cell membrane damage[45]. The decreased disease biomarkers with MDLPs intervention highlight its effect. It was worth noting that the alcohol metabolic process was slightly enriched in the transcriptome GO entry analysis, but none differences such as ethyl glucuronide were found in the metabolomic analysis of ethanol metabolites.

Ethanol treatment did not significantly affect cellular metabolites, as shown by transcriptome GO entry and metabolomics analysis.

Lipid droplets in cells contain neutral lipids, such as triacylglycerols (TAGs) and sterol esters (SE)[47], while lipid droplet-coated proteins are present on the phospholipid membrane on the surface of lipid droplets (Perilipin) and other structural and functional proteins, which regulate lipid droplet homeostasis and intracellular interactions[29]. In this assay, the PLIN4 (Perilipin drop protein 4) gene expression was significantly upregulated, promoting fatty acid transfer from lipid droplets to mitochondria for oxidation, reducing lipid toxicity and alleviating lipid accumulation[48]. Upregulation of mitochondrial oxidative phosphorylation and lipid metabolism-related DEGs suggests MDLPs intervention may enhance biological processes like the tricarboxylic acid cycle, oxidative phosphorylation, fatty acid oxidation, nucleotide synthesis, and amino acid metabolism, leading to changes in the content of oleic acids, nucleotides, amino acids, and flavonoids. Such as the ATPase domain of the ATP4A protein promotes ATP breakdown, releasing energy[49] (Fig. S3).

5. Conclusion

In summary, we concluded that MDLPs intervention significantly mitigated HF-induced lipid accumulation and oxidative stress in HepG2 cells, exhibiting a promising effect on lowering intracellular TC, TG, and ROS levels, as well as improving cell damage. Integrated transcriptome and metabolome indicated that MDLPs mainly altered transcription levels of genes involved in glycerophospholipid metabolism, glycerophospholipid metabolism, and fatty acid degradation, and modulated the abundance of metabolic biomarkers of 4-hydroxynonenal and hydroxylinoleic acid. Both Eth and Non samples exhibited similar alleviating activity. Further, RT-PCR and WB analysis validated that MDLPs regulated key genes involved in lipid metabolism regulation, PPAR, and the FOXO signaling pathway. These results highlight the potential of MDLPs as functional foods and the empowerment of meat proteins in the food industry to improve chronic disease. However, a more detailed profile of MDLPs utilization *in vivo* to mutual verification analysis is warranted in future studies.

Supporting Information

Effects of MDLPs on cell viability of HepG2 cells (Fig. S1); OPLS-DA plot of (A) WT vs. Ind, (B) Ind vs. Eth, and (C) Ind vs. Non groups (Fig. S2); Relative mRNA expression levels of (A) mitochondrial oxidative phosphorylation and (B) glycerophospholipid metabolism-related genes (Fig. S3); Primer sequences for RT-qPCR (Table S1).

Funding

This work was supported by the National Natural Science Foundation of China (Grant No. 32272347), the earmarked fund for China Agriculture Research System (CARS-41), and the Priority Academic Program Development of Jiangsu Higher Education Institution (PAPD)

Notes

The authors declare no competing financial interest.

References

[1] J. Chen, Y. Xiao, D. Li, et al., New insights into the mechanisms of high-fat diet mediated gut microbiota in chronic diseases, iMeta. 2 (2023) e69. https://doi.org/10.1002/imt2.69.

[2] Y. Duan, L. Zeng, C. Zheng, et al., Inflammatory links between high fat diets and diseases, Front. Immunol. 9 (2018) 2649. https://doi.org/10.3389/fimmu.2018.02649.

[3] Y. Ma, H. Xie, N. Xu, et al., Large yellow tea polysaccharide alleviates HFD-induced intestinal homeostasis dysbiosis via modulating gut barrier integrity, immune responses, and the gut microbiome, J. Agric. Food Chem. 72 (2024) 7230–7243. https://doi.org/10.1021/acs.jafc.4c00616.

[4] J. Luo, W. Yan, Z. Chen, et al., Elucidating the anti-obesity phytochemicals in Chenpi and their molecular mechanisms, FSHW. (2025). https://doi.org/10.26599/FSHW.2024.9250204

[5] L. Perez de Isla, L. Masana, R. Argueso, et al., Comments on the 2019 ESC/EAS guidelines for the management of dyslipidemias, Rev. Esp. Cardiol. 73 (2020) 348–353. https://doi.org/10.1016/j.recesp.2019.11.009.

[6] Y. Xiao, D. Yang, H. Zhang, et al., Theabrownin as a potential prebiotic compound regulates lipid metabolism via the gut microbiota, microbiota-derived metabolites, and hepatic FoxO/PPAR signaling pathways, J. Agric. Food Chem. 72 (2024) 8506–8520. https://doi.org/10.1021/acs.jafc.3c08541.

[7] M. Ruscica, N. Ferri, M. Banach, et al., Side effects of statins: from pathophysiology and epidemiology to diagnostic and therapeutic implications, Cardiovasc. Res. 118 (2022) 3288–3304. https://doi.org/10.1093/cvr/cvac020.

[8] F. Guo, H. Xiong, R. Tsao, et al., Green Pea (Pisum sativum L.) Hull polyphenol extract alleviates NAFLD through VB6/TLR4/NF-κB and PPAR pathways, J. Agric. Food Chem. 71 (2023) 16067–16078. https://doi.org/10.1021/acs.jafc.3c02337.

[9] X. Li, B. Zeng, L. Wen, et al., Sea cucumber saponins derivatives alleviate hepatic lipid accumulation effectively in fatty acids-induced HepG2 cells and orotic acid-induced rats, Mar. Drugs 20 (2022) 703. https://doi.org/10.3390/md20110703.

[10] X. Fu, Z. Liu, R. Li, et al., Amelioration of hydrolyzed guar gum on high-fat diet-induced obesity: Integrated hepatic transcriptome and metabolome, Carbohydrate Polymers. 297 (2022) 120051. https://doi.org/10.1016/j.carbpol.2022.120051.

[11] T. Chen, Li, X.Y. Lu, H.D. Jiang, et al., Absorption and excretion of luteolin and apigenin in rats after oral administration of chrysanthemum morifolium extract, J. Agric. Food Chem. 55 (2007) 273–277. https://doi.org/10.1021/jf062088r.

[12] I. Vukelić, D. Detel, L. Batičić, et al., Luteolin ameliorates experimental colitis in mice through ERK-mediated suppression of inflammation, apoptosis and autophagy, Food Chem. Toxicol. 145 (2020) 111680. https://doi.org/10.1016/j.fct.2020.111680.

[13] N. Hayasaka, N. Shimizu, T. Komoda, et al., Absorption and metabolism of luteolin in rats and humans in relation to in vitro anti-inflammatory effects, J. Agric. Food Chem. 66, 43 (2018) 11320–11329. https://doi.org/10.1021/acs.jafc.8b03273.

[14] Z. Zhang, J. Wang, Y. Lin, et al., Nutritional activities of luteolin in obesity and associated metabolic diseases: an eye on adipose tissues, Crit Rev Food Sci Nutr. (2022) 1–15. https://doi.org/10.1080/10408398.2022.2138257.

[15] Y. Luo, S. Chen, J. Zhou, et al., Luteolin cocrystals: Characterization, evaluation of solubility, oral bioavailability and theoretical calculation, J Drug Deliv Sci Technol. 50 (2019) 248–254. https://doi.org/10.1016/j.jddst.2019.02.004.

[16] V. Young, C. Boswell, R. Centeno, et al., DMSO: Applications in plastic surgery, Aesthetic Surgery Journal 25 (2005) 201–209. https://doi.org/10.1016/j.asj.2005.01.015.

[17] Z. Wu, W. Zhang, X. Zhao, et al., Gastrointestinal digestion behavior and bioavailability of greenly prepared highly loaded myofibrillar-luteolin vehicle, Food Res. Int. 187 (2024) 114413. https://doi.org/10.1016/j.foodres.2024.114413.

[18] Z. Wu, X. Zhao, X. Xu, Comparisons between myofibrillar protein–luteolin conjugates fabricated through covalent and noncovalent modification, J. Agric. Food Chem. (2023) acs.jafc.3c01959. https://doi.org/10.1021/acs.jafc.3c01959.

[19] L.-S. Yan, S.-F. Zhang, G. Luo, et al., Schisandrin B mitigates hepatic steatosis and promotes fatty acid oxidation by inducing autophagy through AMPK/mTOR signaling pathway, Metabolism 131 (2022) 155200. https://doi.org/10.1016/j.metabol.2022.155200.

[20] X. Li, Y. Shen, G. Wu, et al., Determination of key active components in different edible oils affecting lipid accumulation and reactive oxygen species production in HepG2 cells, J. Agric. Food Chem. 66 (2018) 11943–11956. https://doi.org/10.1021/acs.jafc.8b04563.

[21] C. Guan, Z. Tan, S. Li, et al., Transcriptomic analysis of Andrias davidianus meat and experimental validation for exploring its bioactive components as functional foods, FSHW. 13 (2024) 166–172. https://doi.org/10.26599/FSHW.2022.9250014.

[22] G. Chen, L. Qi, S. Zhang, et al., Metabolomic, lipidomic, and proteomic profiles provide insights on meat quality differences between Shitou and Wuzong geese, Food Chem. 438 (2024) 137967. https://doi.org/10.1016/j.foodchem.2023.137967.

[23] R. Wang, L. Yao, X. Lin, et al., Exploring the potential mechanism of Rhodomyrtus tomentosa (Ait.) Hassk fruit phenolic rich extract on ameliorating nonalcoholic fatty liver disease by integration of transcriptomics and metabolomics profiling, Food Res. Int. 151 (2022) 110824. https://doi.org/10.1016/j.foodres.2021.110824.

[24] M. Han, Y. Zhang, Y. Fei, et al., Effect of microbial transglutaminase on NMR relaxometry and microstructure of pork myofibrillar protein gel, Eur Food Res Technol. 228 (2009) 665–670. https://doi.org/10.1007/s00217-008-0976-x.

[25] S. Chen, S. Che, S. Li, et al., The combined impact of decabromodiphenyl ether and high fat exposure on non-alcoholic fatty liver disease in vivo and in vitro, Toxicology. 464 (2021) 153015. https://doi.org/10.1016/j.tox.2021.153015.

[26] J. Wang, J. Qu, S. Liu, et al., Tannic acid ameliorates systemic glucose and lipid metabolic impairment induced by low-dose T-2 toxin exposure, J. Agric. Food Chem. 71 (2023) 12574–12586. https://doi.org/10.1021/acs.jafc.3c02934.

[27] S.M. Davidson, M.G. Vander Heiden, METabolic adaptations in the tumor MYCroenvironment, Cell Metabolism. 15 (2012) 131–133. https://doi.org/10.1016/j.cmet.2012.01.005.

[28] H. Zhao, H. Gao, Y. Zhang, et al., Folic acid protects against ethanol-induced hepatic mitophagy imbalance by ROS scavenging and attenuating the elevated hcy levels, J. Agric. Food Chem. 71 (2023) 14276–14288. https://doi.org/10.1021/acs.jafc.3c01851.

[29] L. Li, H. Zhang, Y. Yao, et al., (−)-Hydroxycitric acid suppresses lipid droplet accumulation and accelerates energy metabolism via activation of the adiponectin-AMPK signaling pathway in broiler chickens, J. Agric. Food Chem. 67 (2019) 3188–3197. https://doi.org/10.1021/acs.jafc.8b07287.

[30] F. Guo, H. Xiong, R. Tsao, et al., Multi-omics reveals that green pea (Pisum sativum L.) hull supplementation ameliorates non-alcoholic fatty liver disease via the SHMT2/glycine/mTOR/PPAR-γ signaling pathway, Food Funct. 14 (2023) 7195–7208. https://doi.org/10.1039/D3FO01771K.

[31] S. Hwang, K.W. Chung, Targeting fatty acid metabolism for fibrotic disorders, Arch. Pharm. Res. 44 (2021) 839–856. https://doi.org/10.1007/s12272-021-01352-4.

[32] Schwanhäusser, B., Busse, D., Li, N. et al. Global quantification of mammalian gene expression control. Nature. 473, 337–342 (2011). https://doi.org/10.1038/nature10098

[33] C. Fan, A. Ling-Hu, D. Sun, et al., Nobiletin ameliorates hepatic lipid deposition, oxidative stress, and inflammation by mechanisms that involve the Nrf2/NF-κB axis in nonalcoholic fatty liver disease, J. Agric. Food Chem. 71 (2023) 20105–20117. https://doi.org/10.1021/acs.jafc.3c06498.

[34] D. Shan, J. Wang, Q. Di, et al., Steatosis induced by nonylphenol in HepG2 cells and the intervention effect of curcumin, Food Funct. 13 (2022) 327–343. https://doi.org/10.1039/D1FO02481G.

[35] B. Wehrle-Haller, Structure and function of focal adhesions, Curr. Opin. Cell Biol. 24 (2012) 116–124. https://doi.org/10.1016/j.ceb.2011.11.001.

[36] K.W. Yoon, S. Byun, E. Kwon, et al., Control of signaling-mediated clearance of apoptotic cells by the tumor suppressor p53, Science. 349 (2015) 1261669. https://doi.org/10.1126/science.1261669.

[37]L. Zhang, G.L. Guo, Gut-specific inhibition of PPARα as a novel approach of NAFLD treatment, Hepatology. 77 (2023) 15–17. https://doi.org/10.1002/hep.32592.

[38] S.R. Pyper, N. Viswakarma, S. Yu, et al., PPARα: Energy combustion, hypolipidemia, inflammation and cancer, Nucl Recept Signal. 8 (2010) nrs.08002. https://doi.org/10.1621/nrs.08002.

[39] B. Qian, C. Wang, X. Li, et al., PPARβ/δ activation protects against hepatic ischaemia-reperfusion injury, Liver Int. 43 (2023) 2808–2823. https://doi.org/10.1111/liv.15760.

[40] Z. Ning, X. Guo, X. Liu, et al., USP22 regulates lipidome accumulation by stabilizing PPARγ in hepatocellular carcinoma, Nat Commun. 13 (2022) 2187. https://doi.org/10.1038/s41467-022-29846-9.

[41] M.S. Poornima, G. Sindhu, A. Billu, et al., Pretreatment of hydroethanolic extract of Dillenia indica L. attenuates oleic acid induced NAFLD in HepG2 cells via modulating SIRT-1/p-LKB-1/AMPK, HMGCR & PPAR-α signaling pathways, J Ethnopharmacol. 292 (2022) 115237. https://doi.org/10.1016/j.jep.2022.115237.

[42] Y.-X. Tong, S.-Y. Zhu, Z.-Y. Wang, et al., Sulforaphane ameliorate cadmium-induced blood–thymus barrier disruption by targeting the PI3K/AKT/FOXO1 axis, J. Agric. Food Chem. 72 (2024) 13382–13392. https://doi.org/10.1021/acs.jafc.4c01703.

[43] M.K. Lehtinen, Z. Yuan, P.R. Boag, et al., A conserved MST-FOXO signaling pathway mediates oxidative-stress responses and extends life span, Cell. 125 (2006) 987–1001. https://doi.org/10.1016/j.cell.2006.03.046.

[44] T. Buergel, J. Steinfeldt, G. Ruyoga, et al., Metabolomic profiles predict individual multidisease outcomes, Nat Med 28 (2022) 2309–2320. https://doi.org/10.1038/s41591-022-01980-3.

[45] T. Jiang, L. Dai, P. Li, et al., Lipid metabolism and identification of biomarkers in asthma by lipidomic analysis, Biochim Biophys Acta Mol Cell Biol Lipids. 1866 (2021) 158853. https://doi.org/10.1016/j.bbalip.2020.158853.

[46] Y. Yoshida, A. Umeno, Y. Akazawa, et al., Chemistry of lipid peroxidation products and their use as biomarkers in early detection of diseases, J. Oleo Sci. 64 (2015) 347–356. https://doi.org/10.5650/jos.ess14281.

[47] J. Xie, H. Liu, W. Yin, et al., Zeaxanthin remodels cytoplasmic lipid droplets via β3-adrenergic receptor signaling and enhances perilipin 5-mediated lipid droplet–mitochondrion interactions in adipocytes, Food Funct. 13 (2022) 8892–8906. https://doi.org/10.1039/D2FO01094A.

[48] Z. Li, H. Zhang, Y. Li, et al., Phytotherapy using blueberry leaf polyphenols to alleviate non-alcoholic fatty liver disease through improving mitochondrial function and oxidative defense, Phytomedicine. 69 (2020) 153209. https://doi.org/10.1016/j.phymed.2020.153209.

[49] M. Zhang, Y. Wang, X. Chen, et al., Plasma membrane H^+-ATPase overexpression increases rice yield via simultaneous enhancement of nutrient uptake and photosynthesis, Nat. Commun. 12 (2021) 735. https://doi.org/10.1038/s41467-021-20964-4.